

See discussions, stats, and author profiles for this publication at: <https://www.researchgate.net/publication/7546752>

The Coordination of Uranyl in Water: A Combined Ab Initio and Molecular Simulation Study

ARTICLE *in* JOURNAL OF THE AMERICAN CHEMICAL SOCIETY · NOVEMBER 2005

Impact Factor: 12.11 · DOI: 10.1021/ja0526719 · Source: PubMed

CITATIONS

111

READS

23

4 AUTHORS, INCLUDING:



Daniel Hagberg

Lund University

8 PUBLICATIONS 283 CITATIONS

SEE PROFILE



Gunnar Karlström

Lund University

180 PUBLICATIONS 7,629 CITATIONS

SEE PROFILE

The Coordination of Uranyl in Water: A Combined Quantum Chemical and Molecular Simulation Study

Daniel Hagberg,[†] Gunnar Karlström,[†] Björn O. Roos,^{*,†} and Laura Gagliardi[‡]

Contribution from the Department of Theoretical Chemistry, Chemical Center, University of Lund, P.O. Box 124, S-221 00 Lund, Sweden, and Dipartimento di Chimica Fisica "F. Accascina", University of Palermo, Viale delle Scienze-Parco d'Orleans II, I-90128 Palermo, Italy

Received May 9, 2005; E-mail: Bjorn.Roos@teokem.lu.se

Abstract: The coordination environment of uranyl in water has been studied using a combined quantum mechanical and molecular dynamics approach. Multiconfigurational wave function calculations have been performed to generate pair potentials between uranyl and water. The quantum chemically determined energies have been used to fit parameters in a polarizable force field with an added charge transfer term. Molecular dynamics simulations have been performed for the uranyl ion and up to 400 water molecules. The results show a uranyl ion with five water molecules coordinated in the equatorial plane. The U–O(H₂O) distance is 2.40 Å, which is close to the experimental estimates. A second coordination shell starts at about 4.7 Å from the uranium atom. No hydrogen bonding is found between the uranyl oxygens and water. Exchange of waters between the first and second solvation shell is found to occur through a path intermediate between association and interchange. This is the first fully ab initio determination of the solvation of the uranyl ion in water.

1. Introduction

The identification and characterization of actinide complexes in solution is important for understanding actinide separation and predicting actinide transport in the environment, particularly with respect to the safety of nuclear waste repositories.^{1,2} The uranyl, UO₂²⁺, ion has received considerable interest due to its importance for environmental chemistry of radioactive elements and its role as a benchmark system for larger actinides. A large amount of experimental and theoretical work has thus been published over the years. Direct structural information on the coordination of uranyl in aqueous solution has been obtained mainly by extended X-ray absorption fine structure (EXAFS) measurements,^{3–5} while X-ray scattering studies of uranium and actinide solutions have been more rare.⁶ Only the most recent papers will be referred to in the present discussion.

EXAFS spectra of uranyl cations in acidic aqueous perchlorate and triflate solutions were measured by Sémon et al.,⁴ yielding a number of about five equatorial water molecules bound to uranyl in all cases. EXAFS spectra were also collected

by Allen et al.³ for UO₂²⁺ and NpO₂⁺ as a function of the chloride concentration in aqueous solution. At low chloride concentration, the hydration number and corresponding bond length for UO₂²⁺ are $N = 5.3$ and $R = 2.41$ Å, respectively. The structures of UO₂F_{*n*}(H₂O)_{5–*n*}^{2–*n*} ($n = 3–5$) have been studied by EXAFS and quantum chemistry by Vallet et al.⁵ The typical U–H₂O distance is found to be 2.48 Å. These authors have also studied the structure and bonding in solution of uranyl oxalate complexes.^{7,8} A recent paper by Neuefeind et al.⁶ reported an X-ray scattering experiment on UO₂²⁺ in aqueous solution with the aim to determine its coordination environment. The results indicate, again, that uranyl coordinated to five water molecules is the dominating species, although a small percentage of the uranyl ions are coordinated to four waters. This interpretation depends strongly on the model adopted to describe the charge transfer of electrons from water to the uranyl ion.

Theoretically, various ab initio studies of uranyl with a polarizable continuum model to mimic the environment and/or a number of explicit water molecules have been performed.^{9–13} Some molecular dynamics (MD) studies are also available in the literature. Guilbaud et al.¹⁴ proposed an empirical potential

[†] University of Lund.

[‡] University of Palermo.

- (1) Silva, R.; Nitsche, H. *Radiochim. Acta* **1995**, *70*, 377.
- (2) Grenthe, I.; Fuger, J.; Konings, R.; Lemire, R.; Muller, A.; Nguyen-Trung, C.; Wanner, H. In *Chemical Thermodynamics of Uranium*; Wanner, H., Forest, I., Eds.; North-Holland: Amsterdam, 1992.
- (3) Allen, P. G.; Bucher, J. J.; Shuh, D. K.; Edelstein, N. M.; Reich, T. *Inorg. Chem.* **1997**, *36*, 4676.
- (4) Sémon, L.; Boehme, C.; Billard, I.; Hennig, C.; Lützenkirchen, K.; Reich, T.; Rossberg, A.; Rossini, I.; Wipff, G. *Comput. Phys. Commun.* **2001**, *2*, 591.
- (5) Vallet, V.; Wahlgren, U.; Schimmelpfennig, B.; Moll, H.; Szabó, Z.; Grenthe, I. *Inorg. Chem.* **2001**, *40*, 3516.
- (6) Neuefeind, J.; Soderholm, L.; Skanthakumar, S. *J. Phys. Chem. A* **2004**, *108*, 2733.

- (7) Vallet, V.; Moll, H.; Wahlgren, U.; Szabó, Z.; Grenthe, I. *Inorg. Chem.* **2003**, *42*, 1982.
- (8) Farkas, I.; Bányai, I.; Szabó, Z.; Wahlgren, U.; Grenthe, I. *Inorg. Chem.* **2000**, *39*, 799.
- (9) Clavaguéra-Sarrio, C.; Brenner, V.; Hoyau, S.; Marsden, C. J.; Millié, P.; Dognon, J.-P. *J. Phys. Chem. B* **2003**, *107*, 3051.
- (10) Tsushima, S.; Yang, T.; Suzuki, A. *Chem. Phys. Lett.* **2001**, *334*, 365.
- (11) Vallet, V.; Wahlgren, U.; Schimmelpfennig, B.; Szabó, Z.; Grenthe, I. *J. Am. Chem. Soc.* **2001**, *123*, 11999.
- (12) Hemmingsen, L.; Amara, P.; Ansoborlo, E.; Field, M. *J. Phys. Chem. A* **2000**, *104*, 4095.
- (13) Spencer, S.; Gagliardi, L.; Handy, N.; Ioannou, A.; Skylaris, C.-K.; Willetts, A. *J. Phys. Chem. A* **1999**, *103*, 1831.

for uranyl and used it to simulate the complexation of uranyl by cyclic and acyclic ligands. Hutschka et al.¹⁵ report a series of ab initio calculations on uranyl and Sr^{2+} complexes of $\text{O}=\text{PR}_3$ ligands ($\text{R} = \text{H}, \text{Me}, \text{Ph}$) to assess the role of the substituents R and of the NO_3^- counterions on the intrinsic cation–ligand interaction energy. They also report MD simulations in water on 1:1 and 2:1 complexes of OPR_3 with $\text{UO}_2(\text{NO}_3)_2$, based on an empirical potential.

It seems that, in order to understand the structural and chemical behavior of uranyl (and actinyls in general) in water, it is necessary to go beyond a quantum chemical model of a single uranyl ion in a polarizable continuum medium, eventually with the inclusion of a number of explicit water molecules. A dynamic description of these systems is vital for the understanding of the solvent environment to the doubly charged uranyl ion. It is thus necessary to combine quantum chemical results with molecular dynamics simulations.

Empirical and/or semiempirical potentials are commonly used in most of the existing molecular simulation packages, and they are generated to reproduce information obtained by experiment or to some extent results obtained from theoretical modeling. Simulations using these potentials are therefore accurate only when they are performed on systems similar to those for which the potential parameters were fitted. If one wants to simulate actinide chemistry in solution, this approach is not adequate because there are very little experimental data available for actinides in solution, especially for actinides heavier than uranium. An alternative way is to generate intermolecular potentials fully ab initio from molecular wave functions for the separate entities.

Such an approach (it has been given the name NEMO, Non-Empirical Modeling) has been developed during the last 15 years.^{16,17} It has largely been used to study systems, such as liquid water and water clusters, liquid formaldehyde, acetonitrile, and the solvation of organic molecules and inorganic ions in water. The interested reader is referred to a recent review article¹⁷ by Engkvist for references on the specific applications. Relatively little work with high quality potentials has been performed on the solvation of ions in water (see, however, a recent article by Carillo-Tripp¹⁸ and the thesis of Spångberg¹⁹). This is the first application of such a method to study a highly charged ion in solution. A consequence of the strong coupling between the solvated ion and the water molecules is that a new type of interaction is needed in the potential in order to describe the charge transfer occurring from water to the ion. Such a term has also been included in the present work and will be described in the Method and Details of the Calculations section. The need for a charge transfer term for uranyl was discussed by Hemmingsen¹² and has been included in a (partly empirical) force field recently developed by the group at CEA.⁹

Here, we shall present a purely ab initio study of the structure and dynamics of the water environment to a uranyl ion. The

interaction between uranyl and a water molecule has been studied using accurate quantum chemical methods. The information gained has been used to fit a NEMO potential, which is then used to perform the statistic mechanical simulations. The results confirm the five-coordinated structure of water molecules in the equatorial plane, but show also other interesting structural and dynamical properties of the system.

2. Method and Details of the Calculations

All quantum chemical calculations were performed with the software MOLCAS-6.0.²⁰ The complete active space (CAS) SCF method²¹ was used to generate molecular orbitals and reference functions for subsequent multiconfigurational second-order perturbation calculations of the dynamic correlation energy (CASPT2).^{22–24}

The relativistic effects due to the high atomic number of the uranium atom were taken into account implicitly through the use of Effective Core Potentials (ECPs) derived from high accuracy calculations on the atom. The energy-adjusted uranium ECPs of Küchle et al. were used for this purpose.²⁵ The accompanying basis set of the uranium ECPs was used to describe the valence electron density.²⁵ This basis includes 32 valence electrons on uranium (5s, 5p, 5d, 6s, 6p, 5f, 7s). On the oxygen and hydrogen atoms, the Atomic Natural Orbital type (ANO) basis sets were used, contracted to 4s3p2d and 2s1p on oxygen and hydrogen, respectively.

In our previous studies of the U(V) and U(VI) systems, XUY ($\text{X}, \text{Y} = \text{C}, \text{N}, \text{O}$),^{26–29} we found that it was important to include in the active space the oxygen 2p orbitals and the corresponding UO antibonding orbitals of σ - and π -type. They are hybrid orbitals mixing 5f and 6d of uranium with the 2p orbitals of oxygen. This gives an active space of 12 electrons in 12 orbitals (12/12), which in C_{2v} symmetry are partitioned (4,4,4,0) in the four representations (a_1, b_1, b_2, a_2). This active space was used in this study also. The subsequent CASPT2 calculations were performed with the U(5s5p5d) and O(1s) orbitals frozen.

All of the calculations were performed at the ground state equilibrium geometry of uranyl previously optimized,²⁶ which corresponds to a linear molecule with a uranium oxygen bond distance of 1.705 Å. The structure of the water molecule was optimized using Møller–Plesset second-order perturbation theory (MP2). Five intermolecular potential energy curves between uranyl and water were generated. They are illustrated in Figure 1, where the arrows show the geometry parameters that vary. They were computed at the CASPT2 level of theory, including basis set superposition energy (BSSE) corrections. When referring to the supermolecular system, uranyl plus water, CASPT2 means that an active space including only the uranyl orbitals, as described above, was used, while the occupied water molecular orbitals were kept inactive. In total, CASSCF/CASPT2 calculations were performed for 60 different geometries.

- (14) Guildbaud, P.; Wipff, G. *J. Mol. Struct.* **1996**, 366, 55.
- (15) Hutschka, F.; Dedieu, A.; Troxler, L.; Wipff, G. *J. Phys. Chem. A* **1998**, 102, 3773.
- (16) Wallqvist, A.; Karlström, G. *Chem. Scripta* **1989**, 29A, 131.
- (17) Engkvist, O.; Åstrand, P.-O.; Karlström, G. *Chem. Rev.* **2000**, 100, 4087.
- (18) Carillo-Tripp, M.; Saint-Martin, H.; Ortega-Blake, I. *J. Chem. Phys.* **2003**, 118, 7062.
- (19) Spångberg, D. Cation Solvation in Water and Acetonitrile from Theoretical Calculations. Ph.D. Thesis, Uppsala University, Department of Materials Chemistry, Uppsala University, P.O. Box 538, SE-751 21 Uppsala, Sweden, 2003.

- (20) Karlström, G.; Lindh, R.; Malmqvist, P.-Å.; Roos, B. O.; Ryde, U.; Veryazov, V.; Widmark, P.-O.; Cossi, M.; Schimmelpfennig, B.; Neogrady, P.; Seijo, L. *Comput. Mater. Sci.* **2003**, 28, 222.
- (21) Roos, B. O. In *Advances in Chemical Physics: Ab Initio Methods in Quantum Chemistry-II*; Lawley, K. P., Ed.; John Wiley & Sons Ltd.: Chichester, England, 1987; p 399.
- (22) Andersson, K.; Malmqvist, P.-Å.; Roos, B. O.; Sadlej, A. J.; Wolinski, K. *J. Phys. Chem.* **1990**, 94, 5483.
- (23) Andersson, K.; Malmqvist, P.-Å.; Roos, B. O. *J. Chem. Phys.* **1992**, 96, 1218.
- (24) Roos, B. O.; Andersson, K.; Fülcher, M. P.; Malmqvist, P.-Å.; Serrano-Andrés, L.; Pierloot, K.; Merchán, M. In *Advances in Chemical Physics: New Methods in Computational Quantum Mechanics*; Prigogine, I., Rice, S. A., Eds.; John Wiley & Sons: New York, 1996; Vol. XCIII, pp 219–332.
- (25) Institut für Theoretische Chemie, Universität Stuttgart. ECPs and corresponding valence basis sets. <http://www.theochem.uni-stuttgart.de/>.
- (26) Gagliardi, L.; Grenthe, I.; Roos, B. O. *Inorg. Chem.* **2001**, 40, 2976.
- (27) Gagliardi, L.; Roos, B. O.; Malmqvist, P.-Å.; Dyke, J. M. *J. Phys. Chem. A* **2001**, 105, 10602.
- (28) Gagliardi, L.; Roos, B. O. *Chem. Phys. Lett.* **2000**, 331, 229.
- (29) Gagliardi, L.; Heaven, M. C.; Krogh, J. W.; Roos, B. O. *J. Am. Chem. Soc.* **2005**, 127, 86.

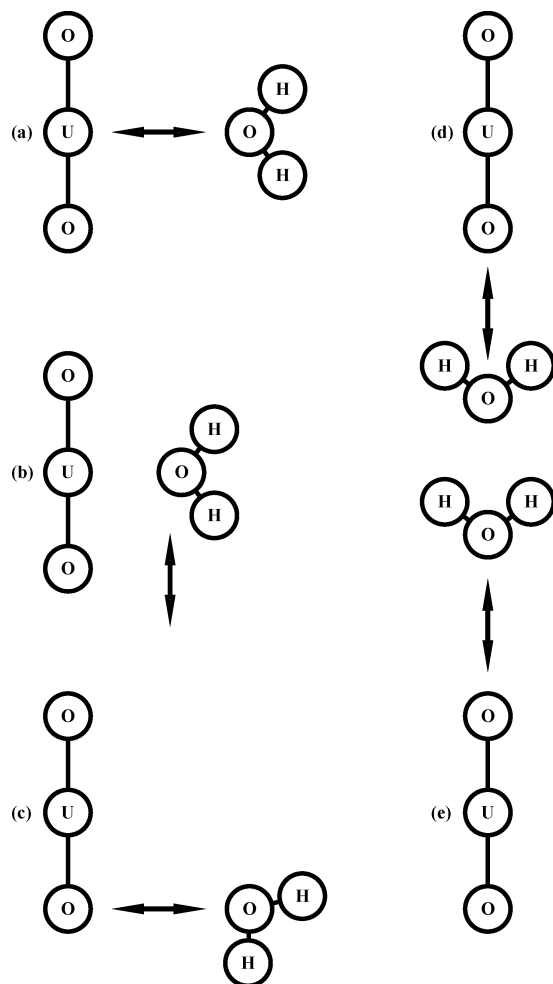


Figure 1. The geometries of the five computed CASSCF/CASPT2 potentials. The arrows show the parameter that is varied.

These calculations produces a geometry for the $\text{UO}_2(\text{H}_2\text{O})^{2+}$ complex according to Figure 1a with all six atoms in a plane, a $\text{U}-\text{O}(\text{H}_2\text{O})$ distance of 2.33 Å, and a binding energy of 270 kJ/mol. We shall discuss these potential curves further in connection with the fitting of the NEMO potential.

The intermolecular potential used in the statistic mechanical simulations was constructed using the NEMO procedure.³⁰ The intermolecular potential will be written as a sum of five terms:

$$E^{\text{tot}} = E^{\text{ele}} + E^{\text{ind}} + E^{\text{disp}} + E^{\text{ere}} + E^{\text{ct}} \quad (1)$$

Normally, only the first four terms are used in the NEMO construct, but here, it is necessary to include an extra term that describes charge transfer from water to uranyl. The starting point for the construction of a NEMO potential is one quantum chemical calculation on each of the interacting molecules. From the wave function of the molecules, a distributed set of charges, dipoles, and quadrupoles are calculated for each of the atoms, although the quadrupoles are replaced by dipoles on atoms close to the site for the quadrupole in actual simulations.³¹ Local polarizabilities are calculated from the wave function using perturbation theory.³² The local multipole and polarizability are used to estimate the electrostatic (E^{ele}) and induction interaction (E^{ind}) between the two molecules. The result of the multipole and polarizability analysis is shown in Table 1. The dispersion interaction (E^{disp}) is calculated using a London-type formula.³⁰ Usually, the dispersion

Table 1. Atomic Coordinates (Å), Interaction Center (IC) Coordinates (Å), Charges (e), Dipoles (eÅ), and Isotropic Polarizabilities (Å³) for the Atoms

	<i>x</i>	<i>z</i>	<i>x</i> _{IC}	<i>z</i> _{IC}	<i>q</i>	<i>μ_x</i>	<i>μ_z</i>	<i>α</i>
U	0.000	0.000	0.000	0.000	2.776	0.000	0.000	1.294
O _{UO₂}	0.000	±1.705	0.000	±1.645	−0.388	0.000	±0.061	1.229
O _{H₂O}	0.000	0.000	0.000	−0.010	−0.868	0.000	−0.176	0.807
H	±0.757	0.586	±0.734	0.571	0.434	±0.078	0.041	0.123

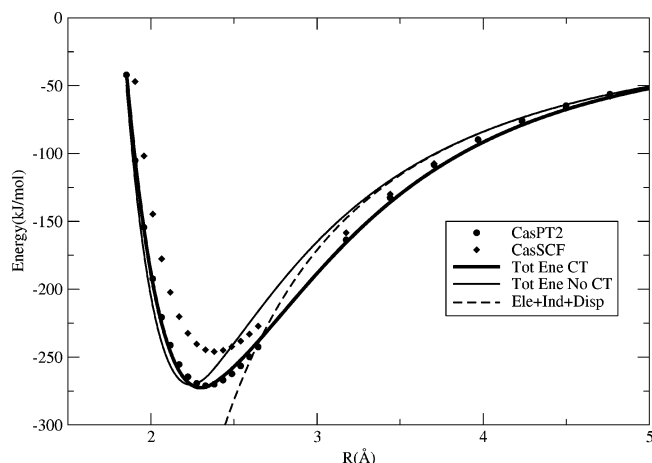


Figure 2. The potential between water and uranyl, with both molecules in the same plane and the water moving in a direction perpendicular to the uranyl axis (a in Figure 1). The dots correspond to the quantum chemical calculation; the lines are the fittings with and without the charge transfer term. The dashed line is the estimate of the interaction energy that comes from the electrostatic, induction, and dispersion terms.

energy is scaled by a factor of 1.89 that is fitted for the basis sets normally used to reproduce the basis set limit dispersion energy. Because we have used different basis sets for the present force field, the scaling factor is not known and both a factor of 1.0 and the old 1.89 are used, as will be explained below.

It now remains to describe the exchange repulsion, E^{ere} , and charge transfer (CT), E^{ct} . To determine these energies, we used the quantum chemical calculations described above. The contributions from the first three terms in eq 1 are subtracted from the total interaction energy, and what remains is the sum of the exchange repulsion and CT terms. This energy is fitted as a sum of interatomic exponential terms, which is used for the final construction of the NEMO potential.

$$E^{\text{ere}} + E^{\text{ct}} = \sum_{i,j} K_{ij}^{\text{ere}} e^{-a_{ij}^{\text{ere}} r_{ij}} - K_{\text{UO}}^{\text{ct}} e^{-a_{\text{UO}}^{\text{ct}} r_{\text{UO}}} \quad (2)$$

where the first term describes E^{ere} and the second, attractive, term describes charge transfer. Values r_{ij} are the distances between atoms i and j . The sum is over all interacting atom pairs i, j . The necessity of including a CT term in the potential has been discussed in earlier work.^{9,12} The term used here is the same as the one suggested by Clavaguera-Sarrio: a simple exponential function depending only on the $\text{U}-\text{O}(\text{H}_2\text{O})$ distance. The importance of the CT term is illustrated in Figure 2, which shows the calculated and fitted potential when the water molecule moves perpendicular to uranyl (Figure 1a).

For some geometries, corresponding to intermediate distances between the water oxygen and the uranyl uranium, the remaining energy is negative when the electrostatic, induction, and dispersion contributions are subtracted from the total interaction energy. The figure shows that, at a distance of about 4 Å, the energy contributions from the electrostatic, induction, and dispersion terms will start to diverge from the CASPT2 curve. This is a consequence of a CT from water to uranyl. The magnitude of the CT (estimated from Mulliken charges) is around 0.15 electrons at 5 au, which corresponds to a CT energy of approximately −20 kJ/mol. The net effect of the charge transfer is that

(30) Wallqvist, A.; Ahlström, P.; Karlström, G. *J. Phys. Chem.* **1990**, *94*, 1649.

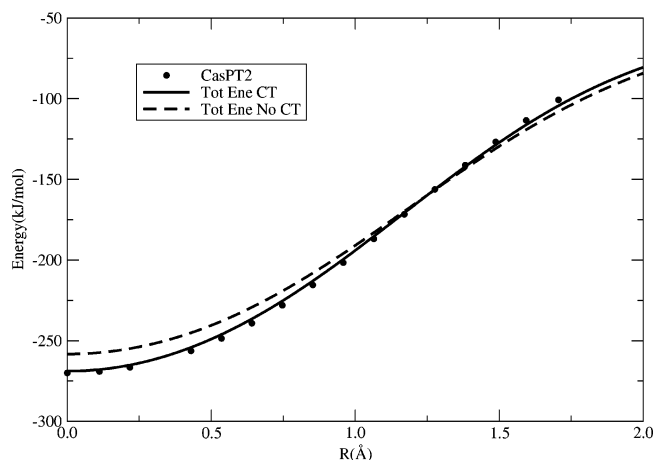
(31) Brdarski, S.; Karlström, G. *J. Phys. Chem. A* **1998**, *102*, 8182.

(32) Karlström, G. *Theor. Chim. Acta* **1982**, *60*, 535.

Table 2. Repulsion Parameters for the Fitted Potentials and for the Water–Water Potential from ref 38 (a is given in \AA^{-1} and K in 10^5 kJ/mol)^a

		UO ₂ H ₂ O	UH	O _{UO₂} O _{H₂O}	O _{UO₂} H	O _{H₂O} O _{H₂O}	O _{H₂O} H	HH
a	no CT	3.8536	3.5989	5.2602	5.1143	2.8087	5.1198	15.5945
a	rep	2.1914	1.9376	4.6073	3.9004			
a	CT	2.1357						
K	no CT	5.605	0.4567	81.70	6.658	0.3252	1.610	7.969
K	rep	6.275	0.0496	30.33	0.2399			
K	CT	5.469						

^a Rows 1 and 4 correspond to the simulation parameters without CT, and the other four rows are the simulation parameters for the fitting, including CT. Rows 2 and 5 represent the repulsion parameters, and rows 3 and 6 are the attractive CT parameters.

**Figure 3.** The potential between water and uranyl, with both molecules in the same plane and the water moving in a direction parallel to the uranyl axis (b in Figure 1). The dots correspond to the quantum chemical calculation; the full line is the fitting with the charge transfer term and the dashed line without.

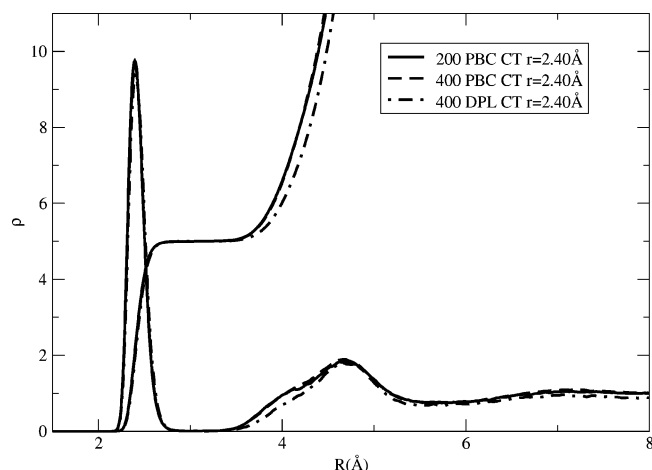
electrons from the hydrogens on water are transferred to the oxygens on the uranyl. Earlier work by Spencer et al. have shown similar electron transfer effects.¹³

The fitting is done as a weighted least-squares optimization. A Boltzmann weight is used with a temperature of $3 \times 10^5 \text{ K}$. The reason for the high temperature is that with an highly attractive interaction energy the configurations outside the potential minimum will otherwise have almost zero weight.

Two fittings were done, with and without the CT term. The electrostatic curve (dashed line) presented in Figure 2 shows that a negative correction is needed for distances shorter than 4 Å. From the figure, it is clear that the quality of the fit is considerably improved by the charge transfer term. The error in the fitting in the energy range of interest for the simulations is smaller than 27 kJ/mol for the fit without the CT term and smaller than 5 kJ/mol when this term is included. The final set of parameters is presented in Table 2. Fitting eq 2 to the CASPT2 energies results in increased repulsion terms, which illustrates the dominance of the CT term in the geometry region a in Figure 1. The spherical form of the CT term will overestimate its effect in the region around the uranyl oxygens. A more complex description of the CT interaction would be needed to remove this effect. Because of the overall goodness of the fit, this was not considered necessary.

The potential created with water moving parallel to the uranyl ion (b in Figure 1) is shown in Figure 3. It is interesting because it shows that the CT term will enhance the preference for the water molecules to be in the equatorial plane. We note also that the fitted potential with the CT term quite accurately reproduces the CASPT2 potential, which gives credibility to the model used to account for charge transfer.

Molecular dynamics (MD) simulations for 200 and 400 water molecules and 1 uranyl ion were performed. Both systems (with 200

**Figure 4.** The U–O radial distribution functions and the integrated radial distribution function for the simulations with 200 (solid line) and 400 (dashed line) water molecules using periodic boundary conditions (PBC) and the CT potential. The same functions are plotted for the droplet (DPL) simulation with 400 waters. The r value is the peak value for the first solvation shell.

and 400 water molecules) were studied with the potential including a charge transfer term, whereas only the MD system with 200 molecules was studied using the less accurate potential. The MOLSIM package³³ was used for the simulations. Periodic boundary conditions (PBC) were used with a spherical interaction cutoff at half the box length, the temperature was kept constant at 300 K, and the particle volume was chosen to be 29.9 \AA^3 . An additional MD (DPL) simulation was performed in order to investigate the effect of different boundary conditions. The ion was kept in the center of the droplet with an external potential that is 0 inside a sphere of radius of 4 Å and grows rapidly for larger radii. We then carried out the simulation with 400 waters that were kept inside another external potential starting at 14.2 Å that defines the droplet. The MD simulations were performed at a constant temperature by scaling the velocities.³⁴ The Verlet algorithm³⁵ was used to solve the equations of motion in the simulations. The choice of the Verlet algorithm, instead of the Gear algorithm, was due to the small dependence of the trajectories on the time step. The system is stable for large displacements due to the large attractive forces in the uranyl–water potential. The time step for the simulations was set to 10^{-16} s , and the simulation with 200 waters ran for $4 \times 10^{-10} \text{ s}$; the simulation with 400 waters ran for 10^{-9} s , while the droplet simulation ran for $2 \times 10^{-10} \text{ s}$. The water–water repulsion was taken from an old fitting and used for the water–water interaction.³⁶

3. Results

Figure 4 shows the radial distribution function (RDF) and the Integrated RDF (IRDF) between U and the water oxygens obtained from the simulation of the uranyl–water systems with the CT term. The results from three different MD simulations are presented. Two simulations are performed for a system with 400 water molecules, and one simulation is performed with 200 water molecules. The results are stable with respect to the choice of simulation method and size of the system. The characteristic feature of the RDF is one major peak at 2.40 Å, which holds five water molecules. This is the maximum of the RDF curve. It could be compared to the minimum obtained for the CASPT2

(33) Linse, P.; Wallqvist, A.; Åstrand, P. O.; Nyman, T. M.; Lobaskin, V.; Carlsson, F. *MOLSIM 3.4.8*; Lund University: Sweden, 2003.

(34) Berendsen, H. J. C.; Postma, J. P. M.; van Gunsteren, W. F.; DiNola, A.; Haak, J. R. *J. Chem. Phys.* **1984**, *81*, 3684.

(35) Swope, W. C.; Andersen, H. C.; Berens, P. H.; Wilson, K. R. *J. Chem. Phys.* **1981**, *76*, 637.

(36) Brdarski, S.; Åstrand, P.; Karlström, G. *Theor. Chem. Acc.* **2000**, *105*, 7.

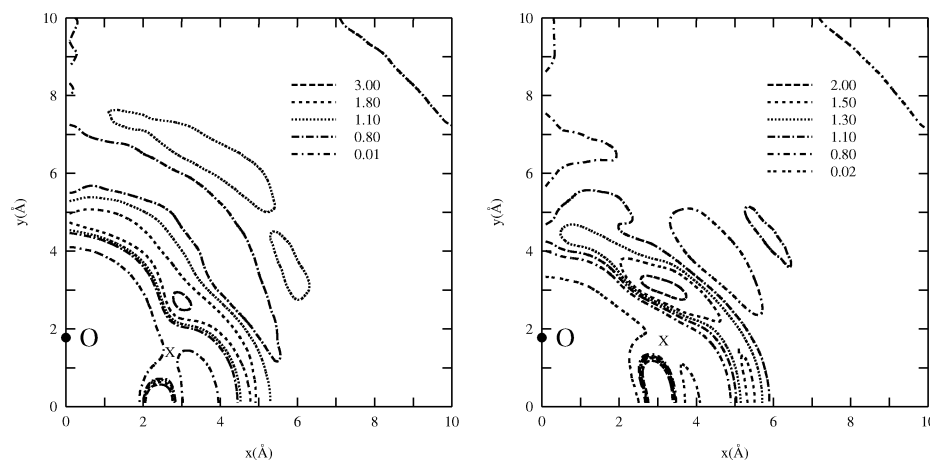


Figure 5. A two-dimensional plot of the water oxygen (left) and water hydrogen (right) distribution functions. The uranium atom is placed in the origin and the uranyl oxygen 1.79 Å up on the y -axis. The X in the figure marks the transition state for an attacking water.

potential with only one water molecule: 2.33 Å. The experimental $\langle r \rangle$ value is 2.41 Å from the EXAFS measurements,³ while X-ray scattering data predict a value of 2.42 Å.⁶ It is clear that the MD simulations are able to predict the structure in the first coordination shell with high accuracy. The average number of water molecules in the first shell is close to 5. The EXAFS data predict a slightly larger value, 5.3, while X-ray scattering predicts a mixture of five and four coordination, with five as the dominating species. The latter result depends, however, strongly on the (problematic) estimate of the electron density to be associated with the water oxygens. The only other MD simulation published so far was based on an empirical potential,¹⁴ which is constructed to yield a five coordination. They obtain an $\langle r \rangle$ value of 2.5 Å, considerably longer than the present result and experiment.

A second coordination shell starts to show up around 4.7 Å outside the uranium atom. Here, the RDF for the two simulations with different boundary conditions (PBC and DPL) differs much more than for the two PBC (200 and 400 waters) simulations, which are almost on top of each other. Very few water molecules are found in the region between the two peaks, indicating that the exchange of water molecules between the shells is a rare event. The rate constant has been estimated from NMR studies to be around 10^6 s^{-1} at 298 K.⁸

More information about the water coordination to UO_2^{2+} can be obtained by plotting the distribution in two dimensions. We show two such plots in Figure 5. The left plot gives the distribution of the water oxygens in an xy -plane, with the uranium atom in the origin and the uranyl oxygen on the y -axis. Due to the cylindrical symmetry, this is actually a three-dimensional picture of the coordination.

Figure 5 shows that the first coordination shell is strongly localized to the equatorial plane, while the peak of the second shell is localized about 3 Å from the uranyl axis and 3 Å from the equatorial plane. The position of the water molecules, in the second shell, is more concentrated in the calotte area around the uranyl axis, and the radial flexibility is more constrained. The right plot shows the hydrogen distribution outside the uranyl ion. The plot has two distinct density peaks that are located at almost the same place as in left plot. Those peaks belong to the same water molecules that give rise to the oxygen peaks in the left plot. The simulation did not produce any strong hydrogen bonds between the uranyl oxygen and a water hydrogen. This

result is at variance with the simulations performed by Guilbaud and Wipff using an AMBER force field.³⁷ They see hydrogen bonding between water and the uranyl oxygens. This is not observed in the present simulations, even if there is a small preference for water molecules in this region to turn the hydrogens closer to the uranyl oxygen atoms. More details will be given below.

The simulations performed without the CT term in the potential do not give results in agreement with experiment. The computed $\langle r \rangle$ value is 2.31 Å, 0.11 Å too short. This effect could have been predicted from the shape of the fitted potential without CT (cf. Figure 2).

The scaling of the dispersion term in the potential (with the factor 1.00 or 1.89 as described in the Method section) hardly effects the RDF. The only noticeable effect of this term is that the probability for finding a water molecule in the region between the two peaks is slightly increased by an increase in the dispersion term. This means that there is an increased probability for water exchange in the simulations performed with the larger scaling factor. It is difficult to estimate the size of this effect. As we shall discuss below, all simulations yield an exchange rate that is larger than what has been measured. We shall therefore focus the analysis on the results obtained from the MD simulation with 400 waters and PBC, using the CT potential without dispersion scaling.

In Figure 6, we present the different radial distribution functions obtained for such a system. The features of the U–O radial distribution function have already been discussed above. Analyzing the RDF between the uranyl oxygen and the water oxygen, a first peak is seen at 3 Å. After that peak, there is a shallow minimum at 3.5 Å. The remaining part of the RDF shows very little structure, except for a small peak at 5.5 Å. We can compare this with the radial distribution function between U and O, which has the five coordinating waters in the first shell at 2.4 Å, and almost no probability of finding a water oxygen between this shell and the second shell at 4.7 Å. The oxygens found in the first peak in the O–O RDF correspond to the oxygen in the first peak in the U–O RDF. This means that the water molecules forming the first solvation shell of the U atom also are the nearest neighbors of the uranyl oxygens, and that the second nearest neighbors of the uranyl oxygens

(37) Guilbaud, P.; Wipff, G. *J. Phys. Chem.* **1993**, *97*, 5685.

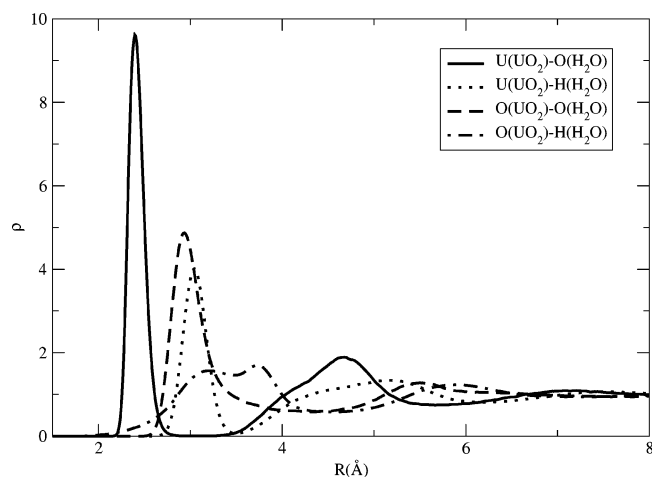


Figure 6. The radial distribution functions for the MD simulation with 400 waters using PBC. The RDFs for all of the four distribution functions between UO_2 and H_2O are plotted.

are oxygen and hydrogen atoms, located about 3 Å outside the uranyl oxygens. The RDF between uranyl oxygen and water hydrogen shows that the density is zero inside 2 Å and increases to a plateau between 3 and 4 Å. There is thus a cavity of about 3 Å outside the uranyl oxygens. The shape of this cavity was already shown in Figure 5. Sometimes, the cavity is rearranged into configurations where there exists a weak hydrogen bond to the uranyl oxygen. The hydrogen bond will then have a length of about 2.0–2.5 Å. These types of configurations are connected to the density line of 0.02 in Figure 5. Thus, two types of structures exist around the uranyl oxygen: a cavity type and a hydrogen bonding type with a preference for the first type.

Figure 5 shows that, beyond the first solvation shell, a minimum is seen in the region between 3 and 4 Å, except at an angle of about 30°, where there is a saddle point marked with an X in Figure 5. This point identifies the geometry of the saddle point for an attacking water molecule attempting to create a six-coordinated complex. An attacking water is supplied by the second solvation shell. The most probable starting place for the attacking water is the peak in the second shell.

A small indication of a third solvation shell is seen in Figure 4. Analyzing the shell structure in Figure 5, it is seen that the first minima along the uranyl axis is located at 6–7 Å, while along the equatorial plane, it is located at 5.5–6 Å and is the second minimum. That gives a slightly distorted third solvation shell. It has a peak at 6–7 Å in the equatorial plane, while along the uranyl axis, the peak is at 7–8 Å. Since the peak and the minimum at 6–7 Å cancel each other in the radial plot Figure 4, a depressed peak and minimum is the result.

The data presented so far deal with the structural properties of the uranyl–water system. However, the molecular dynamics simulations also give information about the dynamics. In Figure 7, we present data illustrating the exchange of water molecules in the first hydration shell of the uranyl ion. The distance between an oxygen atom and the U atom is presented on the y-axis in the figure. The lower black curve shows the distance for the oxygen with the fourth shortest distance to the uranium atom, and the lower gray curve is the same distance to the fifth oxygen. The upper black and gray curves correspond to the sixth and the seventh oxygens. The time for the simulation is presented on the x-axis. At some occasions, the sixth curve approaches the fifth curve, indicating that a water exchange is

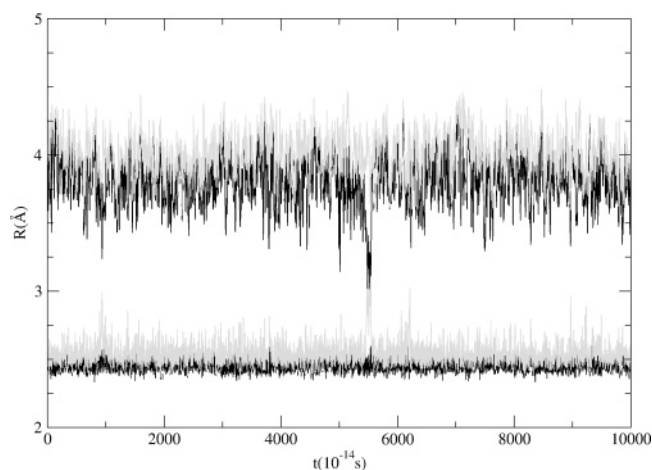


Figure 7. The distance from the uranium atom to oxygen atoms of the coordinated water molecules during a 10^{-10} s simulation. The black line closest to 0 is defined as the fourth oxygen atom in sequence from the uranium atom for a given configuration. The first gray line is the fifth, the second black line the sixth, and the second gray line the seventh oxygen atom, respectively.

about to occur. This does not mean that there is a substitution of a water. The most common behavior is that a sixth water docks to the uranyl–water complex, and after a short time, the water is released again. The water most likely leaves the complex along the same path as the water approached the uranyl ion. There are at least four or five different six-coordination complexes that are visible in Figure 7. There are also configurations where the fifth water tries to leave the complex, resulting in a four-coordinated complex. However, on no occasion is this successful. Looking closer at the figure, one sees that, when a sixth water molecule tries to approach the uranyl complex, the fifth water in the complex is forced to increase its distance to the uranyl ion. The same characteristics are seen when analyzing the MD simulation with 200 waters. In all, there are two successful replacements in the simulation with 400 water molecules in PBC and none for the DPL case. One of the successful water replacements can be seen in the discussed figure at 5500 time units. It is of course impossible to make an estimate of the water exchange rate from so little data, but it seems that the simulations predict a larger value than the experimental results obtained using NMR technique,⁸ which estimated the water exchange rate to be around 10^6 s^{-1} . All events recorded correspond to an associative reaction or something between association (A) and interchange (I). Vallet et al. have computed the energy barriers for the A, I, and D (dissociative) reactions for a $\text{UO}_2(\text{H}_2\text{O})_6^{2+}$ with a continuum solvent model.¹¹ They found the barriers 19(A), 21(I), and 74(D) kJ/mol for the three reactions, a result which is in agreement with the present findings.

4. Conclusions

We have in this work demonstrated that it is possible to construct an accurate interaction potential between water and the uranyl ion fully ab initio, that is, without invoking any empirical parameters. We have also shown that such a potential can be used together with a corresponding description of the water–water interaction to model the behavior of a solvated ion. The structural data obtained in this way are in agreement with available experimental observations. The average number

of coordinated water molecules is five with a U–O bond distance of 2.40 Å, in perfect agreement with the EXAFS and X-ray scattering data. In addition, we have found structural features that have not yet been possible to determine by experiment. Second and third solvation shells are clearly visible. No hydrogen bonding seems to take place between the uranyl oxygens and water molecules.

Exchange of water molecules between the first and second solvation shells of the uranyl ion occurs with a rate constant of about 10^6 s^{-1} . It is not possible to run the simulations for such a long time that one can obtain reasonable statistics for an estimate of this rate. However, the fact that we see a number of attempts for exchange and two successful events during a simulation that lasts for 10^{-9} s indicates that the potential yields a too large rate constant.

The force field has to include an attractive term that describes the charge transfer between water and the uranyl ion. Simulations without this term give erroneous results. It is gratifying that the CT interaction can be modeled with a simple exponential

term. The fitting between the ab initio potential and the parametrized force field with the CT term added is excellent.

The successful modeling of the solvation of the uranyl ion in water demonstrated in the present work, without invoking any empirical information, opens up new possibilities for studying solvation of actinyl ions in water and other solvents. Experimental information is often ambiguous and difficult to obtain. It is therefore important to be able to carry out theoretical simulations, which are independent of any experimental information. This work has shown that such an approach can lead to accurate information about structure and properties of the solvated ions.

Acknowledgment. This work was partially supported by Ministero dell'Università e della Ricerca Scientifica (MIUR), the Swedish Science Research council (VR), and the Swedish Foundation for strategic research (SFF).

JA0526719